



This is the accepted manuscript made available via CHORUS. The article has been published as:

## Enhanced harmonic generation in double-well potentials

G. N. Gibson

Phys. Rev. A **91**, 033411 — Published 25 March 2015

DOI: [10.1103/PhysRevA.91.033411](https://doi.org/10.1103/PhysRevA.91.033411)

# Enhanced harmonic generation in double-well potentials

G. N. Gibson

*Department of Physics, University of Connecticut, Storrs, Connecticut 06269*

## Abstract

Recently, a new 3-level structure, called the  $\Gamma$ -system, has been identified and studied, which shows strong multiphoton coupling and harmonic generation. Under certain circumstances, the  $\Gamma$ -system appears in 1D double well potentials, suggesting that strong multiphoton excitation and harmonic generation may be seen in molecules at favorable internuclear separations, as various aspects of molecules in strong fields can be modeled by 1D potentials. However, even 1D potentials will have additional states, besides the  $\Gamma$ -system, which may interfere with these multiphoton processes. This paper presents numerical solutions to the time-dependent Schrödinger equation (TDSE) of two electrons in a double well potential approximating a dication ( $A_2^{2+}$ ) at various internuclear separations  $R$ . These calculations are compared to 2- and 3-level approximations of the full energy level structure. We show 1) the presence of the  $\Gamma$ -system in the 1D double-well potential; 2) that harmonic generation is enhanced at certain  $R$ ; 3) the enhancement is due to the  $\Gamma$ -system by showing that the 3-level system shows the enhancement, while the 2-level system does not. This goes beyond the work of [M. Berent and R. Parzyński, Phys. Rev. A **82**, 023804 (2010)] by demonstrating that the additional levels in the full TDSE calculation do not disrupt this response. In addition, we investigate a neutral double well potential ( $A_2$ ) with both TDSE and 5-level calculations. While the level structure is not as clear as the dication, enhanced harmonic generation is still present from which we conclude that the  $\Gamma$ -system inherent in the double well potential still allows for a strong multiphoton coupling, even in the presence of other levels. From these calculations, we expect that neutral diatomic molecules at intermediate  $R$  should be a strong source of harmonic generation when exposed to intense laser fields. Indeed, in both charge states, the harmonic radiation is highly non-perturbative, as the power in the harmonics *grows* with harmonic order from 3 to 17, under certain conditions.

PACS numbers: 33.80.Rv, 32.80.Rm, 42.50.Hz

## I. INTRODUCTION

Molecules have a richer response to strong laser fields, compared to atoms due to their additional degrees of freedom [1]. This paper addresses the changes in electronic structure of diatomic molecules as a function of internuclear separation  $R$ , as opposed to the vibrational and rotational motion. The large changes in electronic structure greatly affect how molecules interact with intense laser fields. A well-documented example of this response is the phenomenon of enhanced ionization at a critical  $R$  ( $R_c$ ), where the ionization rate increases dramatically at  $R_c$  [2]. Another aspect of electronic structure of molecules is the presence of charge transfer states which mediate the population of highly-excited electronic states by intense laser fields to a degree not seen in atoms [3]. Population of these excited states can be inferred from the dissociation of molecules into charge asymmetric channels (CAD) [4, 5] or directly through VUV fluorescence measurements [6, 7]. High harmonic generation (HHG) is perhaps the single most important outcome of years of research on atoms and molecules in intense laser fields and should also be strongly affected by the electronic energy level structure of molecules [8].

1D models of atoms and molecules have been quite successful in predicting and explaining their behavior in intense fields [9, 10]. This is perhaps not surprising, at least for linearly polarized light, as the electronic motion is strongly driven along the polarization axis of the applied field. Indeed, enhanced ionization is easily understood in the context of one electron in a double well potential [2]. Some time ago, it also was realized that a 1D double well potential has, under certain circumstances, a 3-level electronic structure with some intriguing properties [3]. If two electrons are placed in a double well corresponding to a net charge of two ( $A_2^{2+}$ ) there is a covalent ground state and a pair of ionic states, otherwise known as charge transfer states. At a large internuclear separation, the ionic states become degenerate and strongly coupled, with a dipole moment approaching the internuclear separation  $R$ . Under these conditions, high order ( $>10$ ) multiphoton coupling becomes very strong, to the point where multiphoton  $\pi$  pulses [3] and adiabatic transfer become possible [11]. This 3-level structure has been dubbed the  $\Gamma$  system [12]. It was suggested and later verified that the  $\Gamma$  system also leads to enhanced harmonic generation [12–14]. Because homonuclear diatomic molecules often follow the predictions from 1D models and they have the charge transfer states which make up the upper levels in the  $\Gamma$  system, homonuclear diatomics at expanded

internuclear separations may be an attractive target for generating harmonic radiation.

The purpose of this paper is two-fold. First, a model 2-electron 1D double well potential ( $A_2^{2+}$ ) is studied in detail. The dication is interesting, as the  $\Gamma$  level structure is quite prominent. However, it is not so clear if the full spectrum of energy levels will interfere with the special properties of the  $\Gamma$  structure. Thus, full TDSE calculations are performed at various  $R$  to see if harmonic generation can be enhanced by varying  $R$  and whether or not any enhancement is due to the  $\Gamma$  system. This is evaluated by performing 2- and 3-level calculations of the lowest lying states: the 2-level calculations should show no special behavior as a function of  $R$ , while the 3-level calculations should capture the essence of the  $\Gamma$  system. Second, 2-electron calculations are performed in a neutral double-well ( $A_2$ ) where the ionic states cross and mix with the covalent states potentially interfering with the  $\Gamma$  structure. While the dication may demonstrate the desirable properties of the  $\Gamma$  system, neutral diatomic molecules are a far more convenient and practical target.

The TDSE calculations for  $A_2^{2+}$  do, in fact, show strong harmonic generation up to 19<sup>th</sup> harmonic (H19) and the level approximations indicate that the strong harmonic response is due to the presence of the  $\Gamma$  structure. Moreover, the TDSE calculations for  $A_2$  show similar enhancements in harmonic generation at intermediate values of  $R$ . Thus, although the ionic and covalent states are strongly mixed in the neutral, the level structure created by the double well is robust enough to show the enhancement in the harmonic generation predicted for the  $\Gamma$  system. Finally, the strong harmonic response of the neutral molecule suggests that the optimal energy level structure for a non-linear process may be more complicated than a simple 3-level system. This raises the more general question of what exactly is the optimal level structure to enhance a particular non-linear process?

While the 1D model may seem like an oversimplification of a diatomic molecule, there are aspects that clearly connect the two. At large  $R$ , the covalent states of  $A_2$  and  $A_2^{2+}$  evolve into the charge symmetric  $A + A$  and  $A^+ + A^+$  dissociation limits. The ionic states evolve into the charge asymmetric  $A^- + A^+$  and  $A + A^{2+}$  dissociation limits. Charge asymmetric dissociation is consistently observed in the strong-field ionization of homonuclear diatomic molecules, such as  $N_2$  [15] and  $I_2$  [4, 5], even though the symmetric channel has a lower energy threshold. This implies that both the covalent and ionic states are active during the strong-field interaction in real molecules. Theoretical work has also demonstrated this strong interaction during ionization [10]. Dissociation of the neutral molecule is obviously not seen

in ionization experiments, although this does not mean that the covalent and ionic states are not active. Indeed, a major motivation of this work is to explore the possibility of probing the strong-field interaction in neutral molecules through low order harmonic generation. Recent experiments [16, 17] have been successful in probing the strong-field ionization of molecules at large R and similar techniques could be applied to harmonic generation.

## II. CALCULATIONS

### A. Numerical methods

The molecular system discussed in the previous section is modeled by a 1-D Hamiltonian consisting of a spatial term,  $H_s$ , and a momentum term,  $H_p$ :  $H(t) = H_s(t) + H_p(t)$ , where  $H_p(p_1, p_2, t) = p_1^2/2 + p_2^2/2$ ,

$$H_s(x_1, x_2, t) = \frac{-Z}{\sqrt{(x_1 - d)^2 + a^2}} + \frac{-Z}{\sqrt{(x_1 + d)^2 + a^2}} + \frac{-Z}{\sqrt{(x_2 - d)^2 + a^2}} + \frac{-Z}{\sqrt{(x_2 + d)^2 + a^2}} + \frac{1}{\sqrt{(x_1 - x_2)^2 + a^2}} + (x_1 + x_2)F(t), \quad (1)$$

$R = 2d$  is the internuclear separation,  $F(t)$  is the electric field strength,  $a$  is a smoothing parameter,  $Z$  is the charge on each atom, and  $x_1, x_2$  ( $p_1, p_2$ ) are the positions (momenta) of the electrons. Atomic units are used throughout this paper. Nuclear motion is assumed to be frozen during the laser pulse. This is similar to the approach used in Ref. [13].

The wavefunctions are propagated in time using standard split-operator techniques. Various grid sizes, space steps, and time steps were compared to test for convergence. In the end, a square grid with  $N = 375$  points was used. The spatial step size is 0.4 au and the time step is 0.03 au. In addition, second order and third order implementations of the split operator were compared [18]. In some case, the second order method showed excessive numerical noise and, so, a third order split operator was used throughout. An absorbing boundary is placed around the edge of the grid to account for ionization.

The five lowest energy levels were found as a function of R in order to calculate dipole couplings and potential energy curves of the model systems, using standard integration in imaginary time, as discussed in [13].

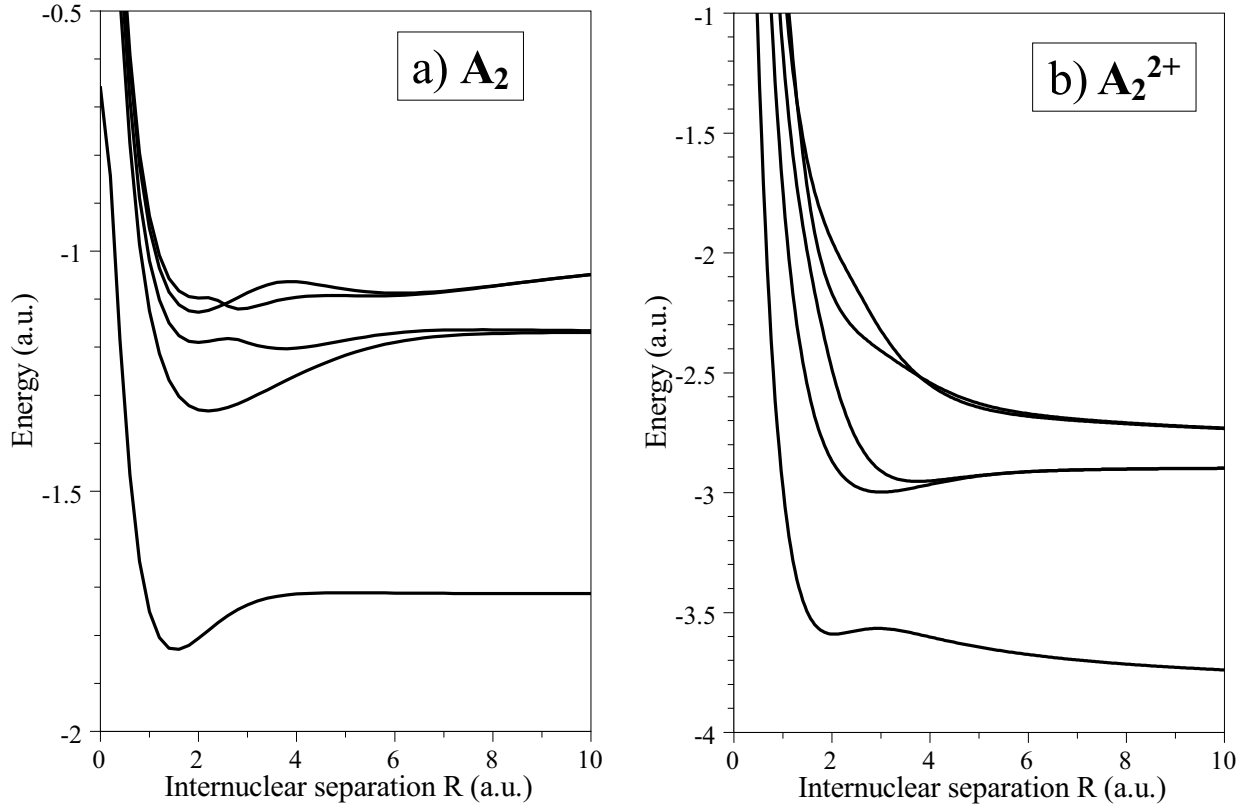


FIG. 1. Five lowest potential energy curves for model diatomic molecules a)  $A_2$  and b)  $A_2^{2+}$ .

Fig. 1a shows these energy levels as a function of internuclear separation,  $R$ , for  $Z = 1$  and  $a = 0.742$ , which roughly corresponds to  $N_2$ , while Fig. 1b shows the results for  $Z = 2$ , corresponding to  $N_2^{2+}$ . Figures 2a and b show the allowed dipole couplings between the various states.

Harmonic generation was calculated using the acceleration form:

$$S_{acc}(\omega) = \left| \int_{-\infty}^{\infty} dt \langle \Psi(t) | -\nabla V | \Psi(t) \rangle e^{i\omega t} \right|^2, \quad (2)$$

where  $\Psi(t)$  is the total time-dependent wavefunction and  $V$  is the potential [19]. When ionization is present, parts of the wavefunction spread to large  $r = \sqrt{x_1^2 + x_2^2}$ . In the length gauge, the calculation is weighted heavily to these extended parts of the wavefunction. However, absorbing boundaries must be used and, thus, the calculated wavefunction deviates significantly from the true wavefunction at large  $r$ . In contrast,  $\nabla V$  is strongly weighted towards small  $r$ . Here, the wavefunction is accurately represented by the calculations, yielding a more consistent and reliable result. Ionization was also measured during the integration

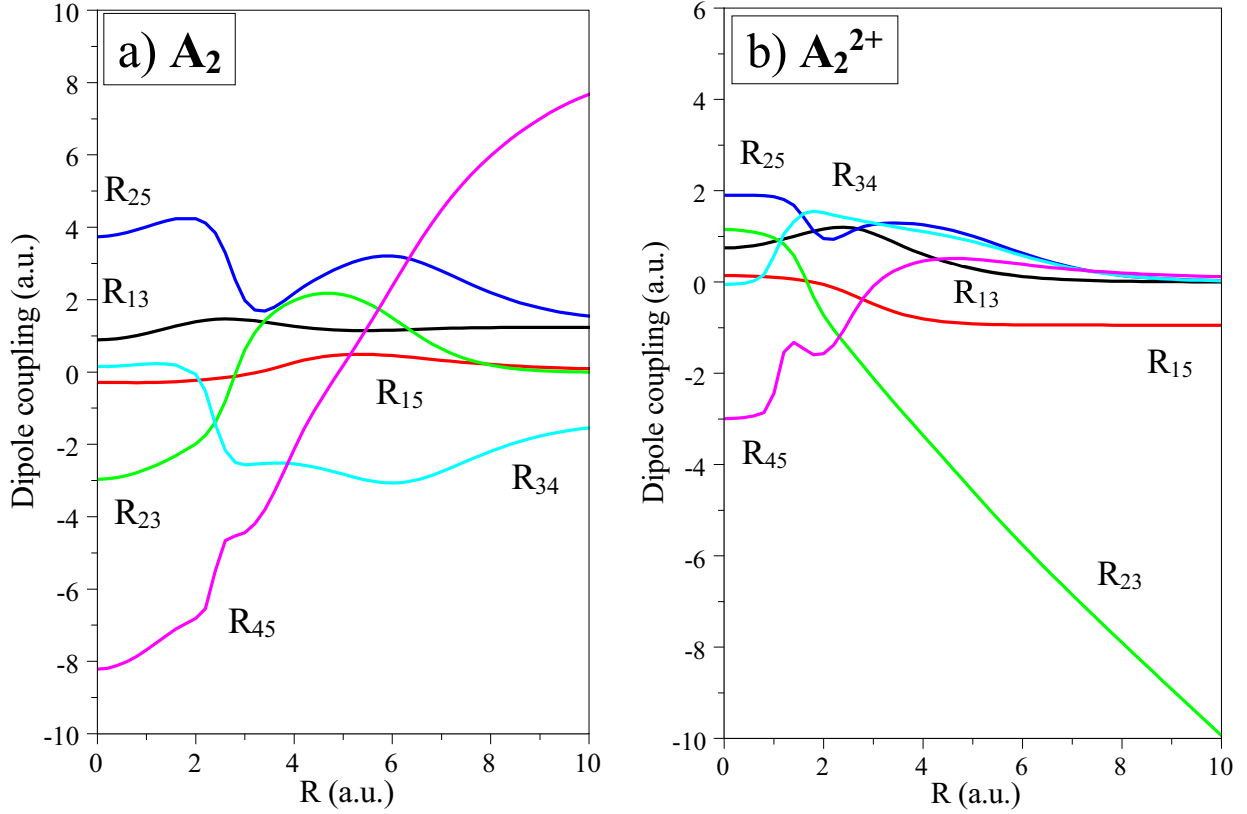


FIG. 2. (color online) Allowed dipole couplings between the various states of a)  $A_2$  and b)  $A_2^{2+}$ .

by simply monitoring the norm of the wavefunction. As parts of the wavefunction reach the absorbing boundary, the norm decreases accordingly.

Besides the full TDSE calculations, harmonic generation was also determined from level approximations, using 2 or 3 levels for  $A_2^{2+}$ . In the 2-level case, the ground and first dipole allowed excited state are included, while in the 3-level case, the ground and first two excited states are included. 5-level calculations were used for  $A_2$  where a clean distinction cannot be made between the covalent and ionic states. In all cases, the energies of the levels and dipole couplings were taken from the full wavefunctions discussed above. The coupled equations describing the level amplitudes were integrated with a second order split operator method. The harmonic generation was calculated in the length gauge, as only the dipole matrix elements enter into the calculation:

$$S_{length}(\omega) = \left| \omega^2 \int_{-\infty}^{\infty} dt \sum_{i>j} R_{ij} (c_i(t) c_j(t)^* + c_i(t)^* c_j(t)) e^{i\omega t} \right|^2, \quad (3)$$

where  $c_i(t)$  are the time-dependent amplitudes in the various levels and  $R_{ij}$  are the dipole couplings between the levels. Ionization cannot be simulated in the level calculations and was not included ad hoc.

## B. Spectroscopy of the potentials

In Fig. 1a, the ionic curves cross the excited state covalent curves, leading to strong mixing. As a result, at any value of  $R$ , it is hard to classify the states based on ionic or covalent character. In the highly ionized molecule (Fig. 1b), the situation is rather different and simpler. The excited covalent curves lie above the ionic ones, and the states retain their ionic or covalent character, as a function of  $R$ .

As can be seen in the Fig. 1b, there is a large energy gap between the ground and first excited states. Moreover, the first excited states are actually a pair of nearly degenerate states with opposite parity and hence are strongly coupled ( $R_{23}$  in Fig. 2b). The gerade ionic state lies slightly higher in energy than the ungerade state, due to the configuration interaction with the gerade ground state. Thus, the dication shows a clear  $\Gamma$  structure with the following correspondence between these states and the levels in the 3-level system: Level 1  $\leftrightarrow$  ground state, Level 2  $\leftrightarrow$  ionic gerade state, and Level 3  $\leftrightarrow$  ionic ungerade state. Starting at about  $R = 3.5$  a.u., the ionic states approach degeneracy and the dipole coupling  $R_{23}$  becomes large and somewhat greater than the coupling to the ground state  $R_{13}$ , the conditions needed for strong multiphoton coupling. As  $R$  increases further,  $R_{23}$  becomes much greater than  $R_{13}$ , which is not favorable for multiphoton interactions [13]. As a result, the strongest multiphoton coupling will occur in the range of  $R = 4$  to 6. Incidentally,  $R_{15}$  approaches a constant value with increasing  $R$  as it becomes the transition dipole of the ground to first excited state of the separated atomic ion, while the rest of the couplings approach zero.

The neutral molecule has a much more complicated interplay between covalent and ionic states, raising the question as to whether the  $\Gamma$  system is manifest. However, certain features are discernible. Only  $R_{23}$  and  $R_{15}$  are trending toward zero as  $R$  increases.  $R_{13}$  connects the ground state to the asymptotic covalent state and evolves into the coupling in the separated atom, like  $R_{15}$  in the dication. Similarly,  $R_{45}$  eventually grows to become the largest coupling at large  $R$ , as this connects the asymptotic ionic states, like  $R_{23}$  in the dication. This reversal



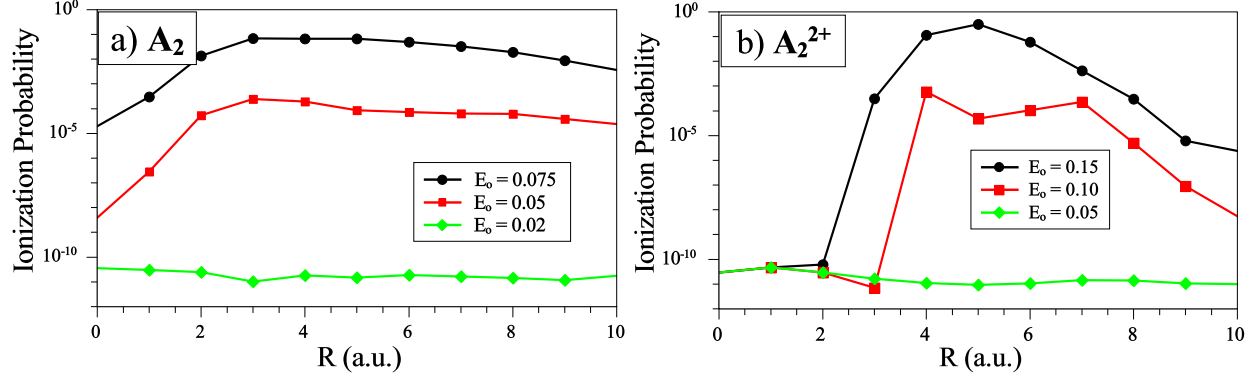


FIG. 3. (color online) Ionization probability as a function of  $R$  for a)  $A_2$  and b)  $A_2^{2+}$  for various electric field strengths  $E_0$ . Note,  $10^{-10}$  is the numerical noise level for ionization probability in these calculations.

comes from the fact that in the neutral, the first covalent states lie below the ionic states, while the opposite is true in the dication, at large  $R$ . Nevertheless, between  $R=6$  to  $7$  a.u.,  $R_{45}$  takes on ionic character and is somewhat larger than  $R_{15}$  and states 4 and 5 are nearly degenerate, suggesting that states 1, 4, and 5 are forming a good  $\Gamma$  system, in this range of  $R$ . As we will see below, strong multiphoton processes in the neutral occur over a wider range of  $R$  and we need to reconsider the implications of Fig. 2a.

### C. Results for $A_2^{2+}$

We first consider the computational results for the dication, as it has been previously studied, to a certain extent [12, 13]. In all of the calculations,  $\omega = 0.057$  a.u., corresponding to a wavelength of 800 nm (1.55 eV photon energy) and the pulse shape is  $E(t) = E_0 \sin^2(t/t_p)$ , with  $t_p = 20$  fs. Fig. 3 shows the total ionization probability as a function  $R$  for three different values of  $E_0$  for both  $A_2$  and  $A_2^{2+}$ . As can be seen for  $A_2^{2+}$ , there is a clear maximum around  $R = 5$  a.u. suggesting enhanced ionization (EI). While the simplest idea of EI corresponds to a single electron in a double well, it was found that even charged molecules (i.e. two electrons in a double well) also show EI, although for rather different reasons [10]. In particular, the coupling to the ionic states was identified as the cause of a maximum in the ionization rate as a function of  $R$ . In any case, the results in Fig. 3 define a reasonable range of intensities to consider, going from minimal to roughly 50% ionization.

Now, we turn to harmonic generation. Fig. 4a shows the harmonic spectrum out to 60 eV

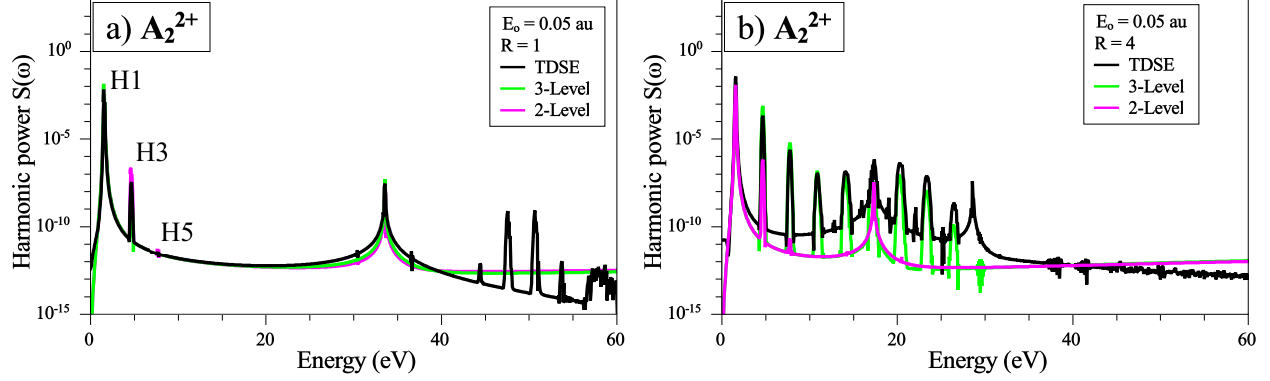


FIG. 4. (color online) Harmonic generation from  $A_2^{2+}$  for a)  $R = 1$ ,  $E_o = 0.05$  and b)  $R = 4$ ,  $E_o = 0.05$ . The positions of the first few harmonics are indicated in a). Various resonant transitions can be seen, such as the 33 eV peak in a).

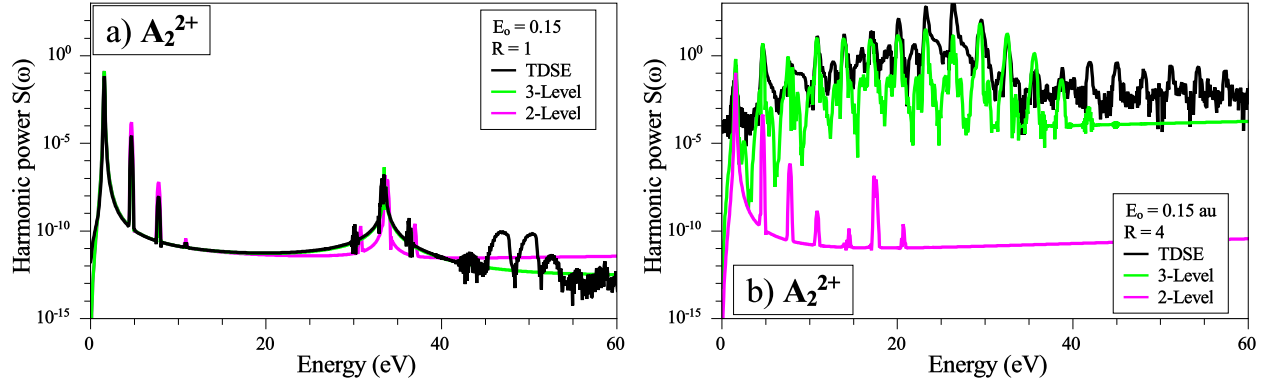


FIG. 5. (color online) Harmonic generation from  $A_2^{2+}$  for a)  $R = 1$ ,  $E_o = 0.15$  and b)  $R = 4$ ,  $E_o = 0.15$ .

at a low field strength of  $E_o = 0.05$  au, corresponding to an intensity of  $8.75 \times 10^{13}$  W/cm<sup>2</sup>, and at a  $R = 1$ . Not surprisingly, there is no harmonic generation beyond H3 and H5. Also shown are the spectra for a 2-level and 3-level approximation. The strong agreement between the 3 calculations shows that only the ground and first dipole allowed excited state are active.

However, the situation changes dramatically for larger  $R = 5$ , shown in Fig. 4b. The 2-level model still shows little harmonic generation beyond H3 and H5. But, now, the 3-level and full wavefunction calculations shows harmonics out to 17. The latter calculations agree reasonably well, except for the higher baseline in the full calculations. This demonstrates that the enhanced harmonics are the result of the  $\Gamma$  structure.

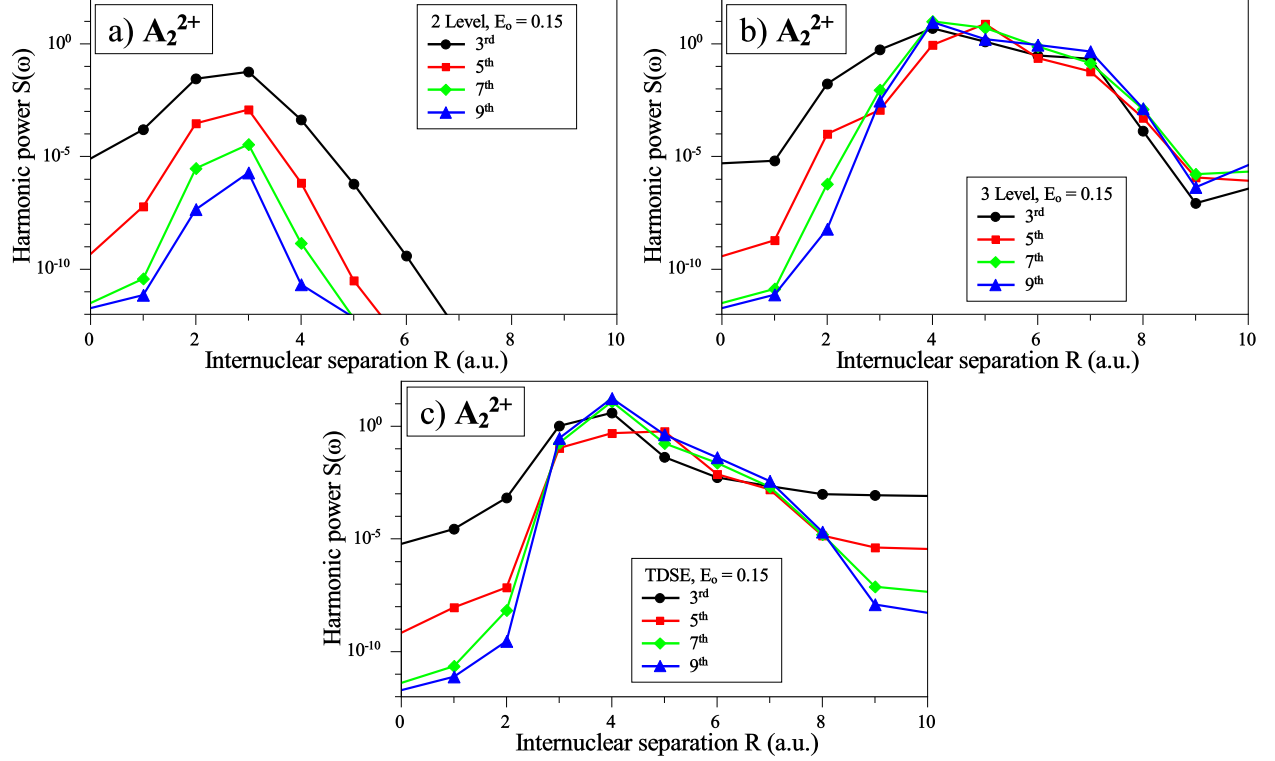


FIG. 6. (color online) Harmonic generation from  $A_2^{2+}$  with  $E_0 = 0.15$  for a) 2-level, b) 3-level, and c) full TDSE calculations.

Figures 5a and b show similar results at a higher field strength  $E_0 = 0.15$  ( $7.88 \times 10^{14}$  W/cm<sup>2</sup>). Again, at small  $R$ , where the  $\Gamma$  structure does not appear, there is still only perturbative harmonic generation, with the intensity falling off rapidly with harmonic order. At  $R = 5$ , the harmonics form a plateau out to H29. It is important to note that this is not due to rescattering. Although rescattering can occur in the full calculations, it will not be present in the 3-level calculation, as there is no ionization. Furthermore, the 3-level and full calculations agree well. Thus, rescattering is not the only way to produce an extended plateau in harmonic generation. Moreover, the plateau seen here starts at H3 and extends from there. In fact, the harmonic power is actually *increasing* with order, at least to H17. This is quite different from the plateau due to rescattering, which only occurs at higher orders and after the efficiency has fallen significantly from the lower orders [20].

Another way to compare the various calculations is to plot the peak power for the first few harmonics as a function of  $R$ , shown in Fig. 6. Fig. 6a displays the results for the 2-level calculation. The harmonics initially rise as a function of  $R$  because the transition energy

between the ground and first allowed excited state is decreasing, making the transition more resonant. However, at after  $R = 3$ , the dipole matrix element  $R_{13}$  starts to decrease, suppressing the harmonics. In addition, the harmonics are well-separated in power, as would be expected from perturbation theory with the higher harmonics always lying well below the lower harmonics. (Below about  $10^{-10}$ , the calculations are in the numerical noise.) The 3-level calculation (Fig. 6b) again shows quite different behavior. The harmonics increase with  $R$  beyond the point that  $R_{13}$  starts to decrease. This is because the ionic state dipole  $R_{23}$  continues to increase and provides the dipole strength for the higher harmonics. Also, the harmonics bunch together in power. This indicates a plateau, if displayed as a spectrum. The bunching, or plateau, extends as far in  $R$  as was considered, although the overall power is decreasing. The exponential decrease in  $R_{13}$  as a function of  $R$  eventually suppresses the harmonic power, even if the behavior remains non-perturbative. Finally, the full calculations (Fig. 6c) are remarkably similar to the 3-level calculation. After the initial rise with  $R$ , the harmonics again bunch together and this plateau extends to  $R = 8$ .

#### D. Results for $A_2$

From the discussion in the previous section, it is clear that the doubly-ionized double well structure shows strong harmonic generation correlated with the emergence of the  $\Gamma$  system. While this was seen before in Ref. [12], we have gone beyond simple 3-level calculations and considered the full TDSE for the double-well potential. Nevertheless, it is clear why the 3-level approximation works for  $A_2^{2+}$ : the ionic states, which form the upper degenerate levels in the  $\Gamma$  system, lie below the covalent states and are well separated in energy. However, the same reasoning does not hold for the neutral double-well. In the neutral, the covalent and ionic states lie closer in energy. As  $R$  changes, the states cross and mix. Thus, a 3-level structure is not so apparent. This complexity is also apparent in the graph of the dipole coupling (Fig. 2a). Nevertheless, a neutral molecule would be a far more useful target for harmonic generation and, so far, we have only established that the  $\Gamma$ -structure is efficient at producing harmonics and that it is manifest in a doubly-ionized double-well potential, under certain conditions. It may be that efficient harmonic generation is inherent in any double-well, even if the energy level structure is not as transparent. Finally, there may be a whole class of potentials that are more efficient at harmonic generation than atomic

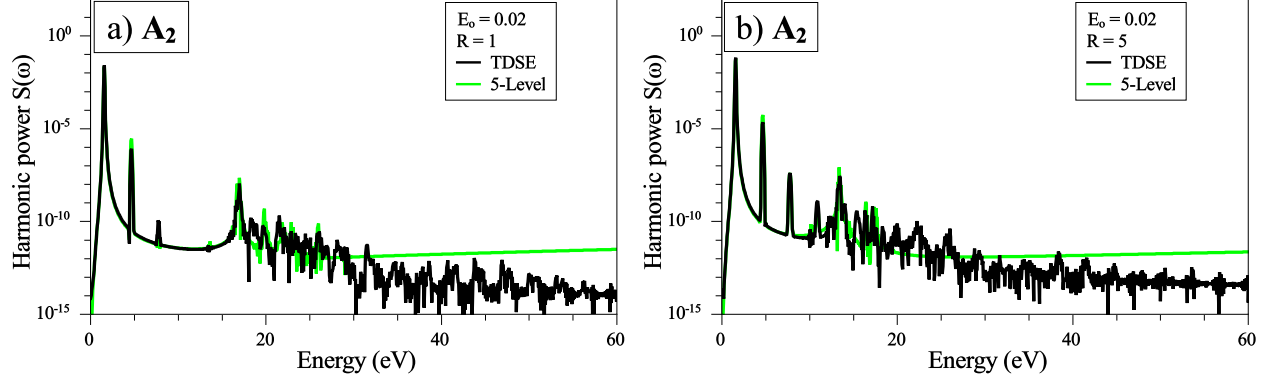


FIG. 7. (color online) Harmonic generation from  $A_2$  for a)  $R = 1$ ,  $E_o = 0.02$  and b)  $R = 5$ ,  $E_o = 0.02$ , using the full TDSE and a 5-Level approximation.

potentials.

As with the dication, we perform numerical calculations on the neutral system by integrating the full TDSE, including ionization, in addition to a 5-level approximation of the system. We do not look at the 2- or 3-level approximations, as it would be fairly arbitrary, in this case, which levels are included, as the excited states defy a clear classification. The 5-level approximation is used to determine whether the large number of more highly-excited and continuum states in the full TDSE play a role harmonic generation.

The range of electric field strengths are chosen in the same way as for the dication. Figure 3a shows the ionization probability as a function of  $R$  for three different values of  $E_o$ , encompassing roughly the same range of ionization as for the dication. While there is still a peak in the ionization probability at about the same value of  $R$ , the peak is much broader and extends towards larger  $R$ . This will be discussed more, below. The parameters of the calculation, including the pulse shape, are the same as for the dication.

As before, we calculate the harmonic spectrum at low intensity and small values of  $R$ , shown in Fig. 7a. As expected, the harmonic radiation falls off rapidly with harmonic order. In addition, the 5-level and full TDSE calculations agree quite well, demonstrating that only the low lying levels are active in the harmonic generation. Figure 7b shows the results for  $R = 5$ . Here, the harmonic generation is significantly higher, but the harmonics still fall with increasing order.

At a higher electric field strength  $E_o = 0.075$ , the situation changes. Note, this is not an unreasonable value to choose, as the ionization probability is still only 50%. Of course,

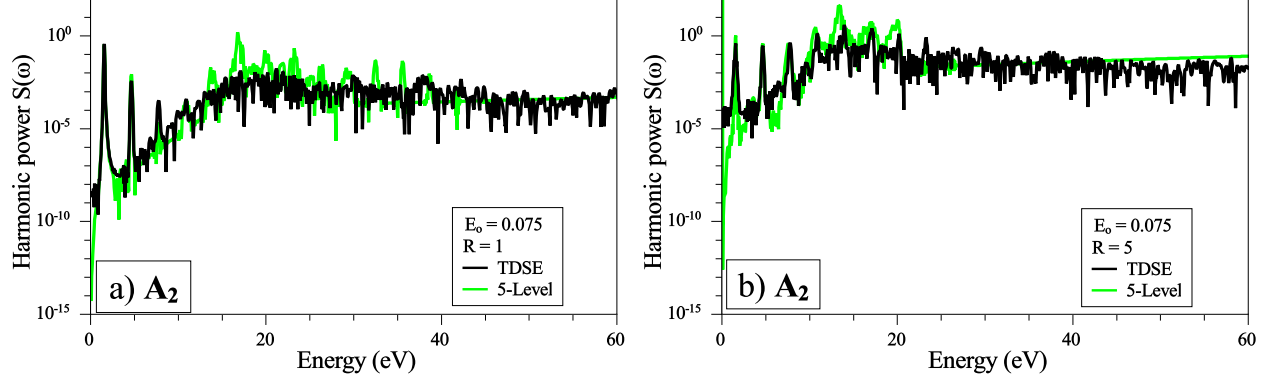


FIG. 8. (color online) Harmonic generation from  $A_2$  for a)  $R = 1$ ,  $E_o = 0.075$  and b)  $R = 5$ ,  $E_o = 0.075$ , using the full TDSE and a 5-Level approximation.

the overall harmonic signal is much stronger, but at  $R = 1$ , the harmonics still fall off with increasing harmonic order. At  $R = 5$ , though, we enter into the non-perturbative regime in which the harmonics increase with order at least up to H9. While not as dramatic as in the dication, it is still very unusual to have the harmonics increase in this way. Also, as before, the 5-level approximation matches the full calculations quite well, implying that the higher-lying states and ionization do not play a role in this behavior.

Finally, we show the harmonic power as a function of  $R$  for the lowest order harmonics (H3-H11) in Fig. 9 for both the 5-level and full TDSE calculations, similar to Fig. 6 for the dication. As in Fig. 6, the harmonics in Fig. 9 initially increase with  $R$  and eventually fall off at large  $R$ . However, the falloff is much more gentle for the neutral molecule. The 5-level and TDSE calculations show similar behavior, although the TDSE results are smoother, perhaps due to the additional levels present. Nevertheless, the harmonics still bunch together, indicating a non-perturbative response. From this, we conclude that neutral molecules at an intermediate value of  $R$  should show enhanced harmonic generation with a non-perturbative response, in that higher harmonics can be stronger than the lower order harmonics.

### E. Comparison of $A_2$ to $A_2^{2+}$

We finish by addressing one last question: why does the enhanced harmonic generation in the neutral double-well extend over a wider range of  $R$ , compared to the dication? As we

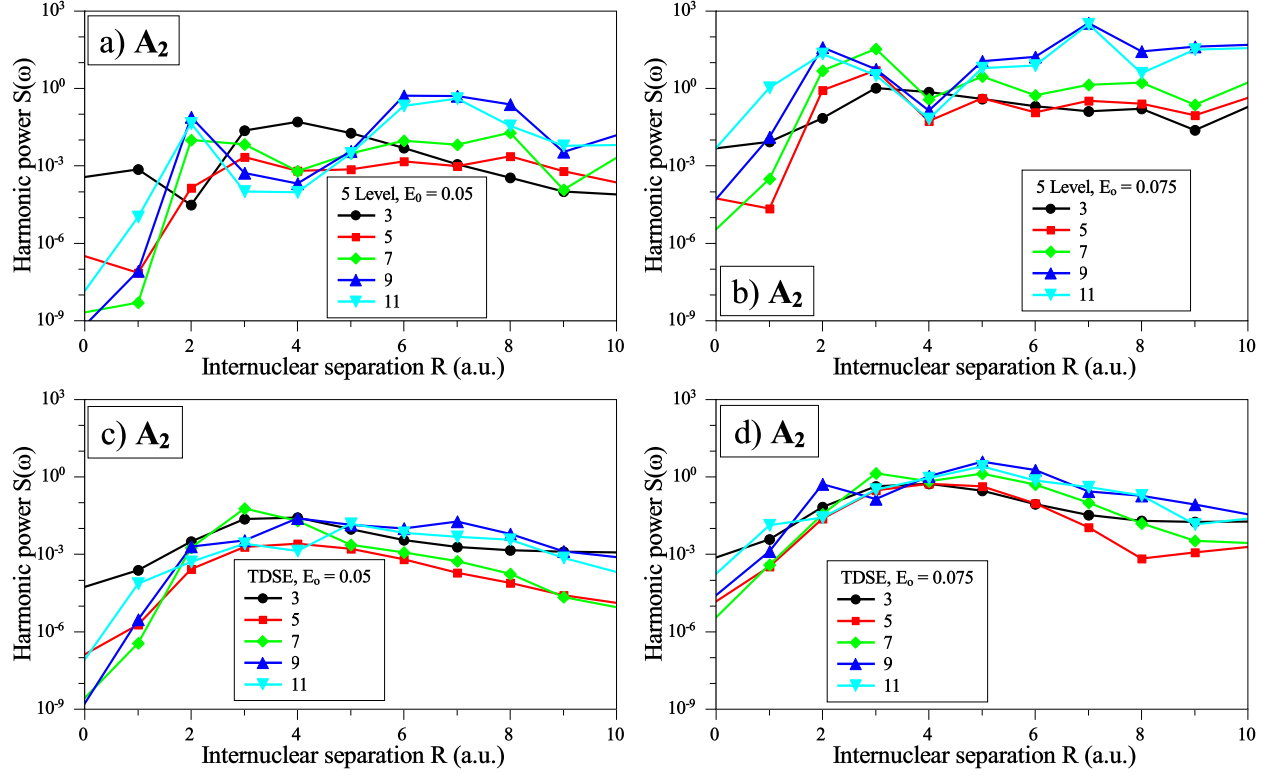


FIG. 9. (color online) Harmonic generation from  $A_2$  for a)  $E_o = 0.05$  and b)  $E_o = 0.075$ , using a 5-Level approximation and c)  $E_o = 0.05$  and d)  $E_o = 0.075$ , using the full TDSE calculations.

discussed, the dication shows a clear  $\Gamma$ -structure over the range of  $R$  that shows enhanced harmonic generation. In addition, the covalent and ionic states in  $A_2^{2+}$  decouple rapidly with  $R$ , as seen by  $R_{25}$  and  $R_{34}$  decaying to zero with  $R$ . In contrast, even though the ionic and covalent states eventually separate in the neutral, they remain coupled as  $R_{25}$  and  $R_{34}$  do not go to zero (See Fig. 10).  $R_{15}$  does approach zero, effectively cutting off the ground state from the ionic system (levels 4 and 5 in the neutral), as in the dication. However,  $R_{13}$  does not go to zero, keeping the ground state coupled to the covalent levels. The covalent levels, in turn, stay coupled to the ionic states through  $R_{25}$  and  $R_{34}$ . Thus, the strong modulation of the degenerate ionic states can still contribute their strong multiphoton coupling to the system as a whole.

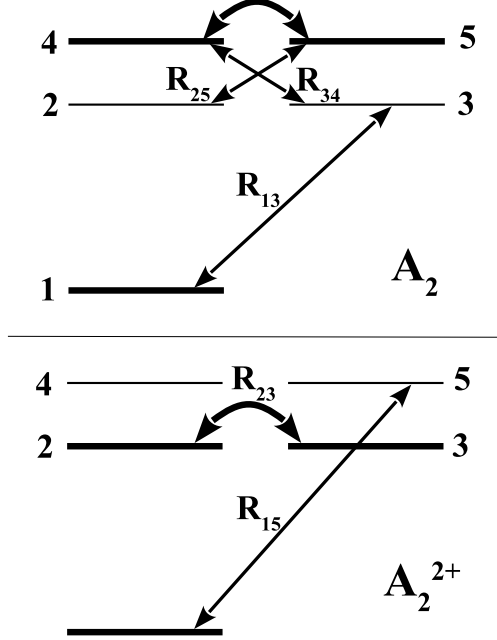


FIG. 10. Level diagrams for  $A_2$  and  $A_2^{2+}$  showing the non-zero dipole couplings at large  $R$ . The thick lines correspond to the  $\Gamma$ -system.

### III. CONCLUSION

We studied in detail harmonic generation from a doubly-ionized double-well potential, confirming and extending previous predictions and analytic results. Indeed, harmonic generation from a doubly-ionized double-well potential is greatly enhanced at intermediate values of the internuclear separation where a 3-level  $\Gamma$ -structure is known to exist. However, to experimentally test these predictions, a neutral diatomic molecule would be far more convenient, although it is not clear if such a system would show enhanced harmonic generation. Thus, we also performed numerical simulations of harmonic generation from a neutral double-well potential and found qualitatively similar behavior to the doubly-ionized system, despite the fact that the neutral does not display a clean  $\Gamma$  system. Thus, this raises an interesting question about what exactly is the most favorable energy level and coupling scheme to enhance harmonic generation or, more generally, any particular non-linear response.



#### IV. ACKNOWLEDGMENTS

I would like to acknowledge support from the NSF under Grant No. PHY-1306845.

- 
- [1] G. N. Gibson, L. Fang, and B. Moser, *Progress in Ultrafast Intense Laser Science V*, K. Yamanouchi (Ed.) (Springer, Berlin, 2010), pg. 1.
  - [2] T. Seideman, M.Y. Ivanov, and P.B. Corkum, Phys. Rev. Lett. **75**, 2819 (1995).
  - [3] G. N. Gibson, Phys. Rev. Lett. **89**, 263001 (2002).
  - [4] G. N. Gibson, M. Li, C. Guo, and J. P. Nibarger, Phys. Rev. A. **58**, 4723 (1998).
  - [5] J. P. Nibarger, M. Li, S. Menon, and G. N. Gibson, Phys. Rev. Lett. **83**, 4975 (1999).
  - [6] G. Gibson, T. S. Luk, A. McPherson, K. Boyer, and C. K. Rhodes, Phys. Rev. A **40**, 2378 (1989).
  - [7] R. N. Coffee and G. N. Gibson, Phys. Rev. A **69**, 053407 (2004).
  - [8] For example, O. Smirnova, Y. Mairesse, S. Patchkovskii, N. Dudovich, D. Villeneuve, P. Corkum, and M. Yu. Ivanov, Nature **460**, 972 (2009).
  - [9] W.-C. Liu, J.H. Eberly, S.L. Haan, and R. Grobe, Phys. Rev. Lett. **83**, 520 (1999).
  - [10] I. Kawata, H. Kono, Y. Fujimura, and A.D. Bandrauk, Phys. Rev. A **62**, 031401(R) (2000).
  - [11] G. N. Gibson, Phys. Rev. A **72**, 041404(R) (2005).
  - [12] M. Berent and R. Parzyński, Phys. Rev. A **82**, 023804 (2010).
  - [13] G. N. Gibson, Phys. Rev. A **67**, 043401 (2003).
  - [14] H. K. Avetissian, B. R. Avchyan, and G. F. Mkrtchian, Phys. Rev. A **77**, 023409 (2008).
  - [15] J. P. Nibarger, S. V. Menon, and G. N. Gibson, Phys. Rev. A **63**, 053406 (2001)
  - [16] H. Chen, V. Tagliamonti, and G. N. Gibson, Phys. Rev. Lett. **109**, 193002 (2012).
  - [17] H. Chen, V. Tagliamonti, and G. N. Gibson, Phys. Rev. A **86**, 051403(R) (2012).
  - [18] M. R. Hermann and J. A. Fleck, Jr., PRA **38**, 6000 (1988); A. D. Bandrauk and H. Shen, Can. J. Chem. **70**, 555 (1992).
  - [19] K. Burnett, V. C. Reed, J. Cooper, and P. L. Knight, Phys. Rev. A **45**, 3347 (1992).
  - [20] A. L’Huillier and Ph. Balcou, Phys. Rev. Lett. **70** 774 (1993).